NASA TM X-516

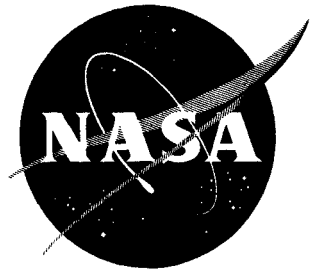

TECHNICAL MEMORANDUM

X-516

STATIC LONGITUDINAL STABILITY AND CONTROL CHARACTERISTICS AT A MACH NUMBER OF 2.01 OF A HYPERSONIC MISSILE CONFIGURATION HAVING ALL-MOVABLE WING AND TAIL SURFACES

By Ross B. Robinson and Gerald V. Foster

Langley Research Center
Langley Field, Va.

NATIONAL AERONAUTICS AND SPACE ADMINISTRATION
WASHINGTON
April 1961

[redacted]

NATIONAL AERONAUTICS AND SPACE ADMINISTRATION

TECHNICAL MEMORANDUM X-516

STATIC LONGITUDINAL STABILITY AND CONTROL CHARACTERISTICS AT A MACH NUMBER OF 2.01 OF A HYPERSONIC MISSILE CONFIGURATION HAVING ALL-MOVABLE WING AND TAIL SURFACES*

By Ross B. Robinson and Gerald V. Foster

SUMMARY

An investigation has been made to determine the longitudinal stability and control characteristics at a Mach number of 2.01 of a hypersonic missile configuration having all-movable cruciform wings and tails. The effects of deflecting the wing and tail surfaces individually and in combination were determined for an angle-of-attack range of about -1° to 27°. A limited amount of roll control data was also obtained. The investigation was made in the Langley 4- by 4-foot supersonic pressure tunnel at a Reynolds number of about 7.42×10^{6} based on the model length.

Deflections of the wing and tail controls in combination provided the highest trim values of angle of attack and normal force but at the cost of high values of drag. The highest values of trim lift-drag ratio were obtained by using the tail controls alone.

Differential deflection of the vertical tails provided a suitable means of roll control, whereas differential deflection of the vertical wings was less desirable because of a nonlinear variation of rolling moment with angle of attack and a large adverse yawing moment.

AUTHOR

INTRODUCTION

In order to obtain information on the stability and control characteristics of configurations that offer promise as hypersonic missiles, an investigation of a family of missile models has been undertaken. The initial phases of the investigation are reported in reference 1 for a

*Title, Unclassified.

Mach number of 2.01 and in reference 2 for Mach numbers from 2.29 to 4.65. The control characteristics at Mach numbers of 2.01, 4.65, and 6.8 of two configurations, one having low-aspect-ratio cruciform wings with trailing-edge flap controls and one having a flared afterbody and all-movable cruciform controls, are presented in reference 3. This investigation has been extended to determine the stability and control characteristics of the basic body of the family of missile models in combination with the trailing-edge flap controls of reference 3 which are used as tails and all-movable cruciform wing controls at a Mach number of 2.01. Results are presented with a limited analysis.

SYMBOLS

The force and moment coefficients are referred to the body-axis system except the lift and drag coefficients, which are referred to the wind-axis system. For the basic data, the moment reference point is located at 50 percent of the body length.

C_N	normal-force coefficient,	$\frac{\text{Normal force}}{qA}$
C_L	lift coefficient,	$\frac{\text{Lift}}{qA}$
C_A	axial-force coefficient,	$\frac{\text{Axial force}}{qA}$
C_D	drag coefficient,	$\frac{\text{Drag}}{qA}$
C_m	pitching-moment coefficient,	$\frac{\text{Pitching moment}}{qAd}$
C_n	yawing-moment coefficient,	$\frac{\text{Yawing moment}}{qAd}$
C_l	rolling-moment coefficient,	$\frac{\text{Rolling moment}}{qAd}$
C_Y	side-force coefficient,	$\frac{\text{Side force}}{qA}$
L/D	lift-drag ratio,	C_L/C_D
q	free-stream dynamic pressure, lb/sq ft	

A	cross-sectional area of body base, sq in.
d	diameter of body base, in.
x	longitudinal distance rearward of nose, in.
l	body length, in.
r	body radius, in.
α	angle of attack, deg
δ_w	all-movable-wing-control deflection, positive when trailing edge is down or to the left, deg
δ_t	tail deflection, positive when trailing edge is down or to the left, deg

Subscripts:

b	base
trim	value at trim conditions
h	horizontal
v	vertical

MODEL DESCRIPTION

Geometric details of the model are presented in figure 1 and table I. Coordinates of the forebody are presented in table II. The model consisted of a 5-caliber forebody (a round nose followed by a conical section) that faired into a 5-caliber cylindrical afterbody section. Two sets of cruciform all-movable controls were attached to the model. These controls were flat plates with rounded leading edges and blunt trailing edges. One set of controls (the all-movable wings) had a modified 70° delta planform with the control hinge line located at the 46.7-percent body station and at 68.7 percent of the root-chord line of the control. The other set of controls (the horizontal and vertical tails) had rectangular planforms with the hinge line located at the 93.3-percent body station and at 33 percent of the root-chord line of the control.

[redacted]

APPARATUS, TESTS, AND CORRECTIONS

Tests were made in the Langley 4- by 4-foot supersonic pressure tunnel at a Mach number of 2.01. Force and moment data were measured through the use of a six-component internal strain-gage balance. The conditions under which tests were conducted are presented in the following table:

Stagnation temperature, $^{\circ}F$	100
Stagnation pressure, lb/sq in. abs	12
Reynolds number based on body length	7.42×10^6

The stagnation dewpoint was maintained sufficiently low to prevent condensation effects in the test section.

The angles of attack were corrected for the deflection of the balance and sting under load. The base pressure was measured, and the axial force was adjusted to a base pressure equal to free-stream static pressure. The variation of base axial-force coefficient with angle of attack is shown in figure 2.

Estimated maximum probable errors in the results, based on 0.5 percent of the maximum balance loads, are as follows:

C_N, C_L ($\alpha = 0^{\circ}$)	±0.120
C_A, C_D ($\alpha = 0^{\circ}$)	±0.008
C_m	±0.110
C_n	±0.110
C_l	±0.033
C_Y	±0.120

It is believed that the actual errors are somewhat less than these estimated errors because the loads on the balance were well within the balance limits for all but the highest angles of attack. The angles of attack are correct within $\pm 0.2^{\circ}$ and the control deflection angles, within $\pm 0.1^{\circ}$.

PRESENTATION OF RESULTS

The results of the investigation are presented in the following figures:

SUMMARY OF RESULTS

All the configurations had the nonlinear variations of C_N and C_m with α that are typical of a configuration with small low-aspect-ratio lifting surfaces (figs. 3 and 4). The large increase in stability with increasing angle of attack presents a difficult longitudinal-control problem. A forward location of the moment center, necessary to insure stability at low angles of attack, results in large values of C_m to be trimmed by the controls. To reduce these trimming requirements with a more rearward moment-center location would result in the configuration's becoming unstable at low angles of attack. The increments of C_m produced by deflection of the wings and tails were nearly constant with angle of attack, although the increments in C_N and C_L due to large deflections of the wings diminished rapidly at high angles of attack (fig. 4).

Deflecting the wing with the horizontal tail fixed at -20° provided the highest values of α_{trim} and $C_{N,trim}$ but at the cost of high values of $C_{D,trim}$ and resultingly low values of $(L/D)_{trim}$. (Compare data from figs. 5 and 6.) The tails alone (fig. 5) were more effective as controls than the wings alone (fig. 6(a)) and nearly as effective as the wings used in combination with a tail deflection of -10° (fig. 6(b)). The highest values of $(L/D)_{trim}$ and lowest values of drag were obtained by using the tails alone for control (fig. 5).

Differential deflection of the vertical tails for roll control provided approximately constant values of C_l throughout the angle-of-attack range, with small values of favorable C_n at low angles of attack that increased with increasing angle of attack (fig. 7(a)). The vertical wings appeared to be less desirable for roll control because of the nonlinear variation of rolling moment with angle of attack and the large nonlinear variations of adverse yawing moment obtained (fig. 7(b)).

Langley Research Center,
National Aeronautics and Space Administration,
Langley Field, Va., January 18, 1961.

REFERENCES

1. Robinson, Ross B.: Wind-Tunnel Investigation at a Mach Number of 2.01 of the Aerodynamic Characteristics in Combined Angles of Attack and Sideslip of Several Hypersonic Missile Configurations With Various Canard Controls. NACA RM L58A21, 1958.

2. Turner, Kenneth L., and Appich, W. H., Jr.: Investigation of the Static Stability Characteristics of Five Hypersonic Missile Configurations at Mach Numbers From 2.29 to 4.65. NACA RM L58D04, 1958.

3. Spearman, M. Leroy, and Robinson, Ross B.: Longitudinal Stability and Control Characteristics at Mach Numbers of 2.01, 4.65, and 6.8 of Two Hypersonic Missile Configurations, One Having Low-Aspect-Ratio Cruciform Wings With Trailing-Edge Flaps and One Having a Flared Afterbody and All-Movable Controls. NASA TM X-46, 1959.

TABLE I.- GEOMETRIC CHARACTERISTICS OF MODEL

Body:	
Length, in.	30.00
Diameter, in.	3.00
Maximum cross-sectional area, sq in.	7.07
Length-diameter ratio	10.00
Fineness ratio of forebody	5.00
Moment-center location, percent body length	50.00
All-movable wings:	
Exposed area, per pair, sq in.	15.70
Total span, in.	7.42
Root chord, in.	6.40
Tip chord, in.	0.33
Leading-edge sweep angle, deg	70
Thickness, in.	0.19
Hinge-line location, percent body length	46.7
Hinge-line location, percent root chord	68.7
Tails:	
Exposed area, per pair, sq in.	8.04
Total span, in.	5.68
Root chord, in.	3.00
Tip chord, in.	3.00
Leading-edge sweep angle, deg	0
Thickness, in.	0.19
Hinge-line location, percent body length	93.3
Hinge-line location, percent root chord	33.3

TABLE II.- COORDINATES OF FOREBODY

x/l	r/l
0	0
.0088	.0099
.200	.0321
.233	.0358
.267	.0392
.300	.0421
.333	.0445
.367	.0465
.400	.0480
.433	.0491
.466	.0497
.500	.0500

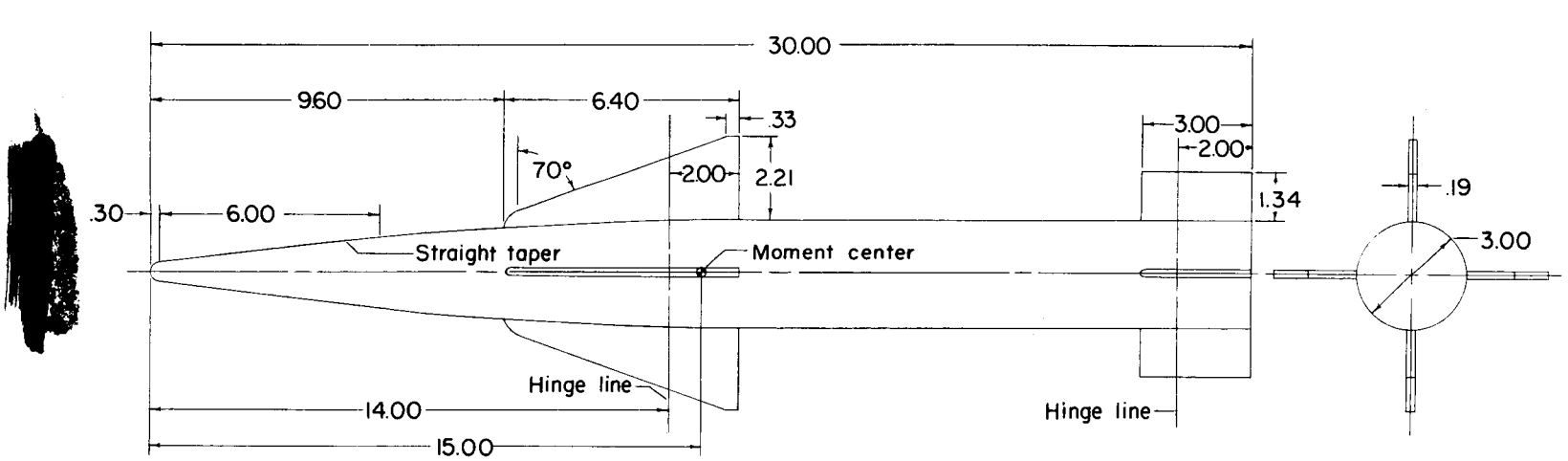

Figure 1.- Details of model. All dimensions are in inches.

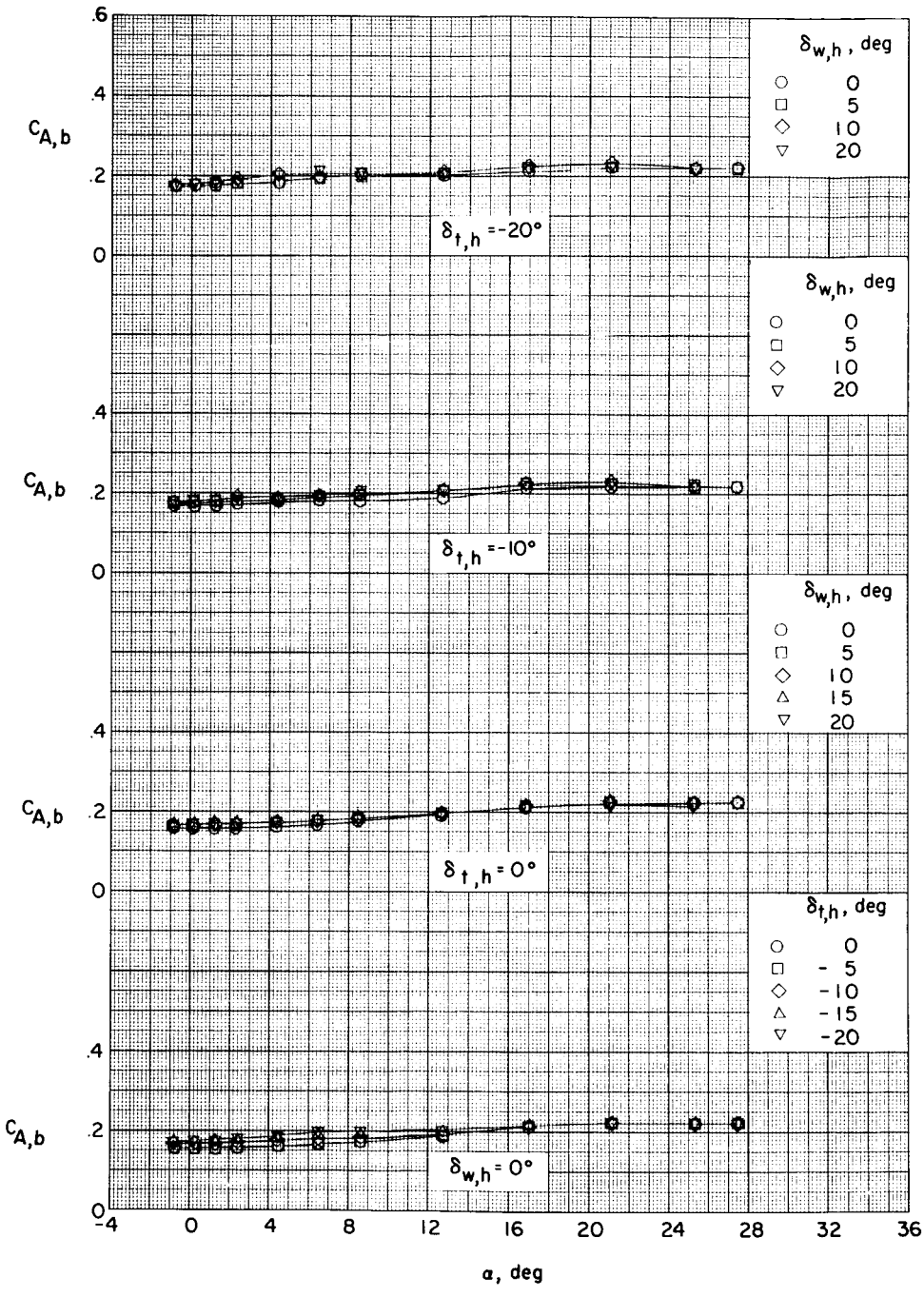

Figure 2.- Variation of base axial-force coefficient with angle of attack. $\delta_{w,v} = 0^{o}$; $\delta_{t,v} = 0^{o}$.

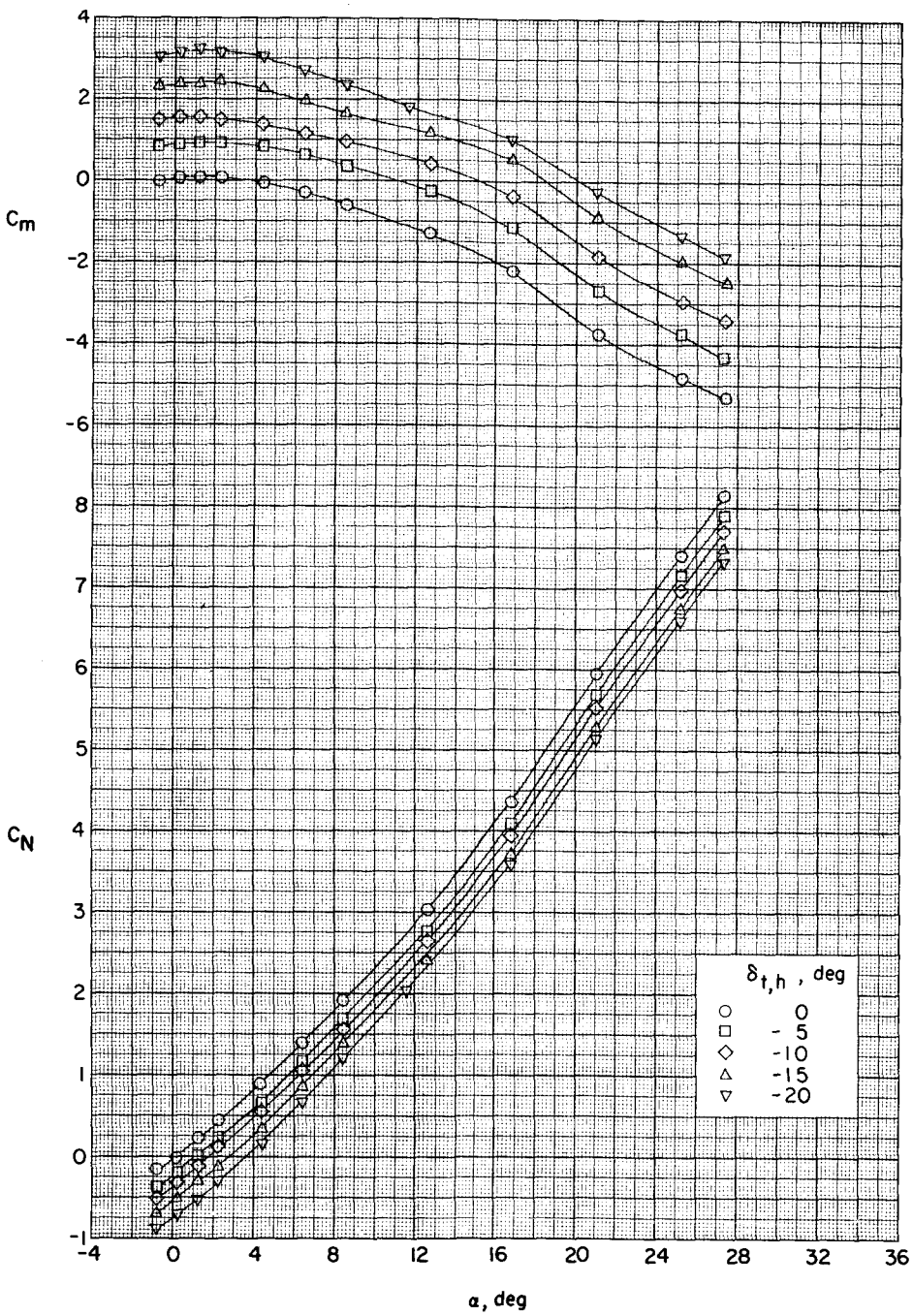

Figure 3.- Effect of horizontal-tail-control deflection on aerodynamic characteristics in pitch. $\delta_w = 0^o$; $\delta_{t,v} = 0^o$.

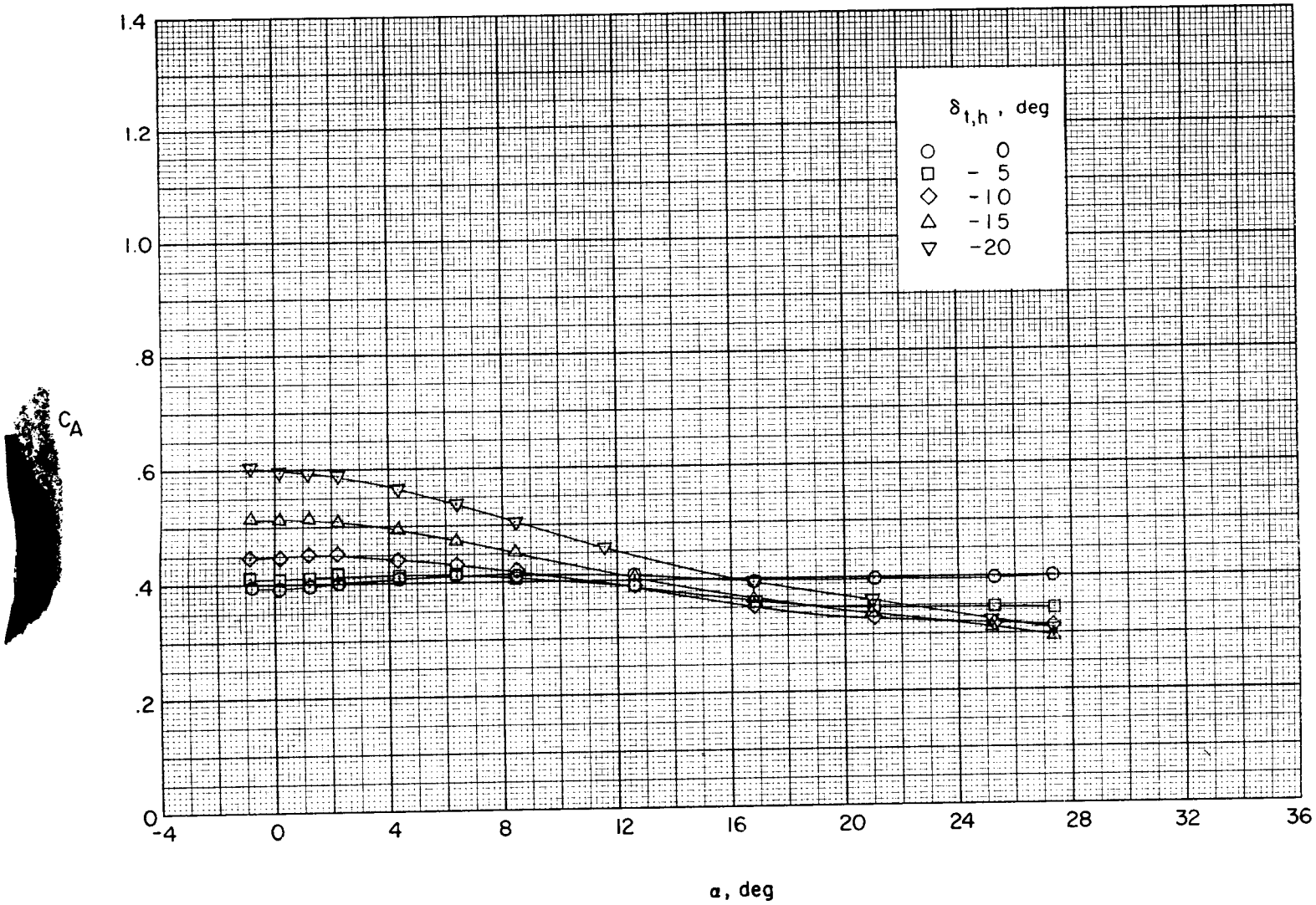

Figure 3.- Continued.

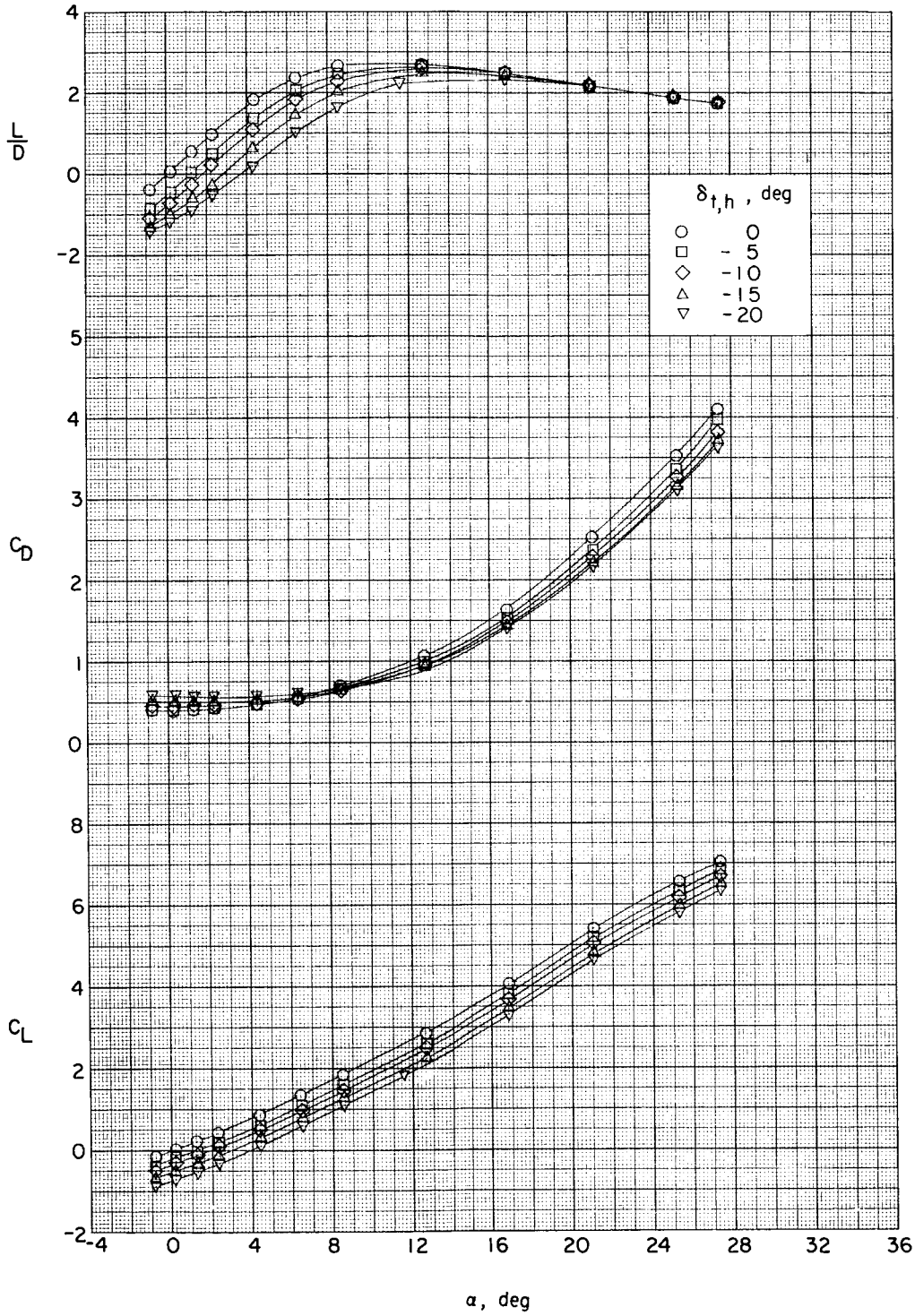

Figure 3.- Concluded.

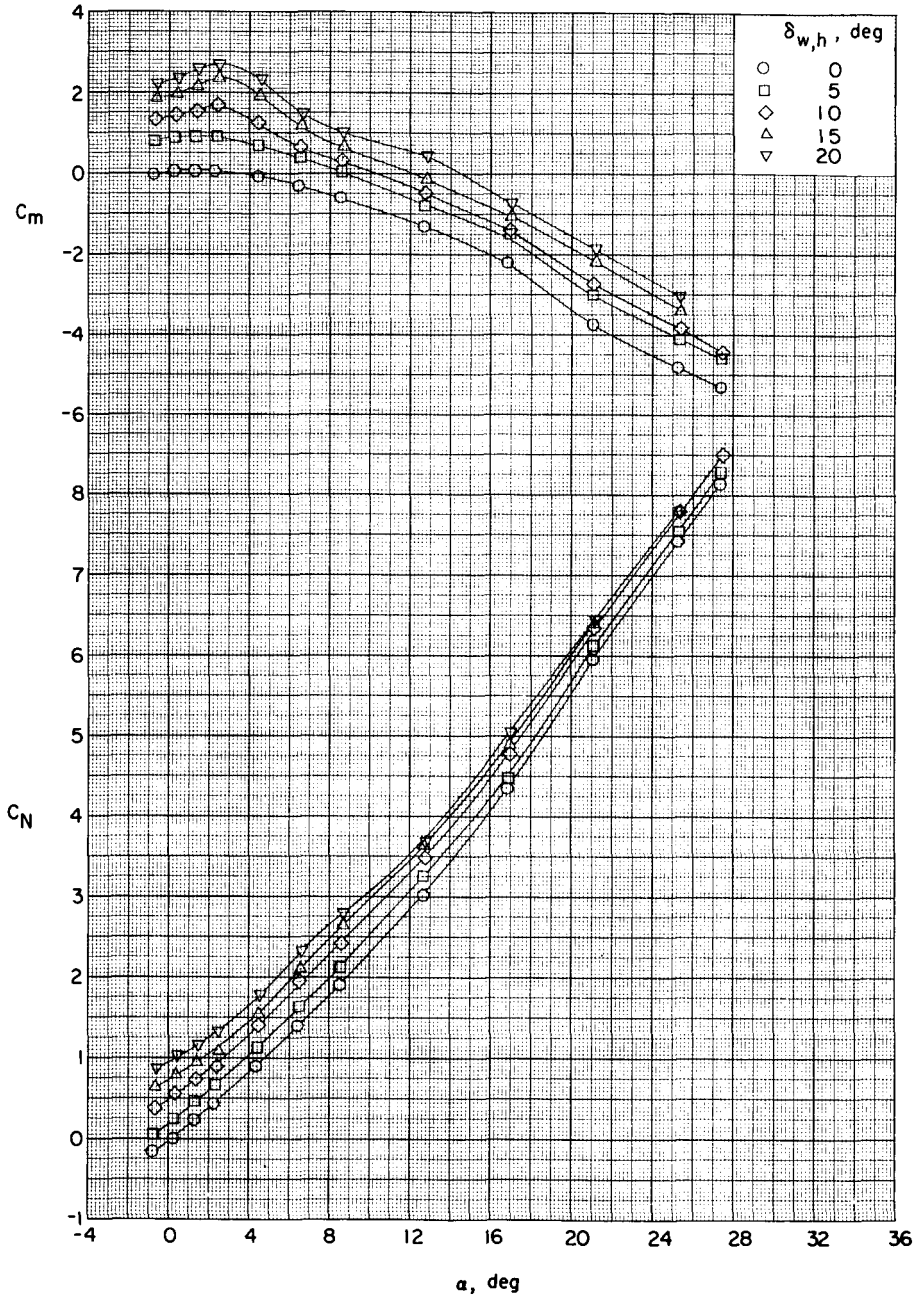

(a) $\delta_{t,h} = 0^{\circ}$.

Figure 4.- Effect of wing-control deflection on aerodynamic characteristics in pitch for various deflections of the horizontal tail. $\delta_{w,v} = 0^{\circ}$; $\delta_{t,v} = 0^{\circ}$.

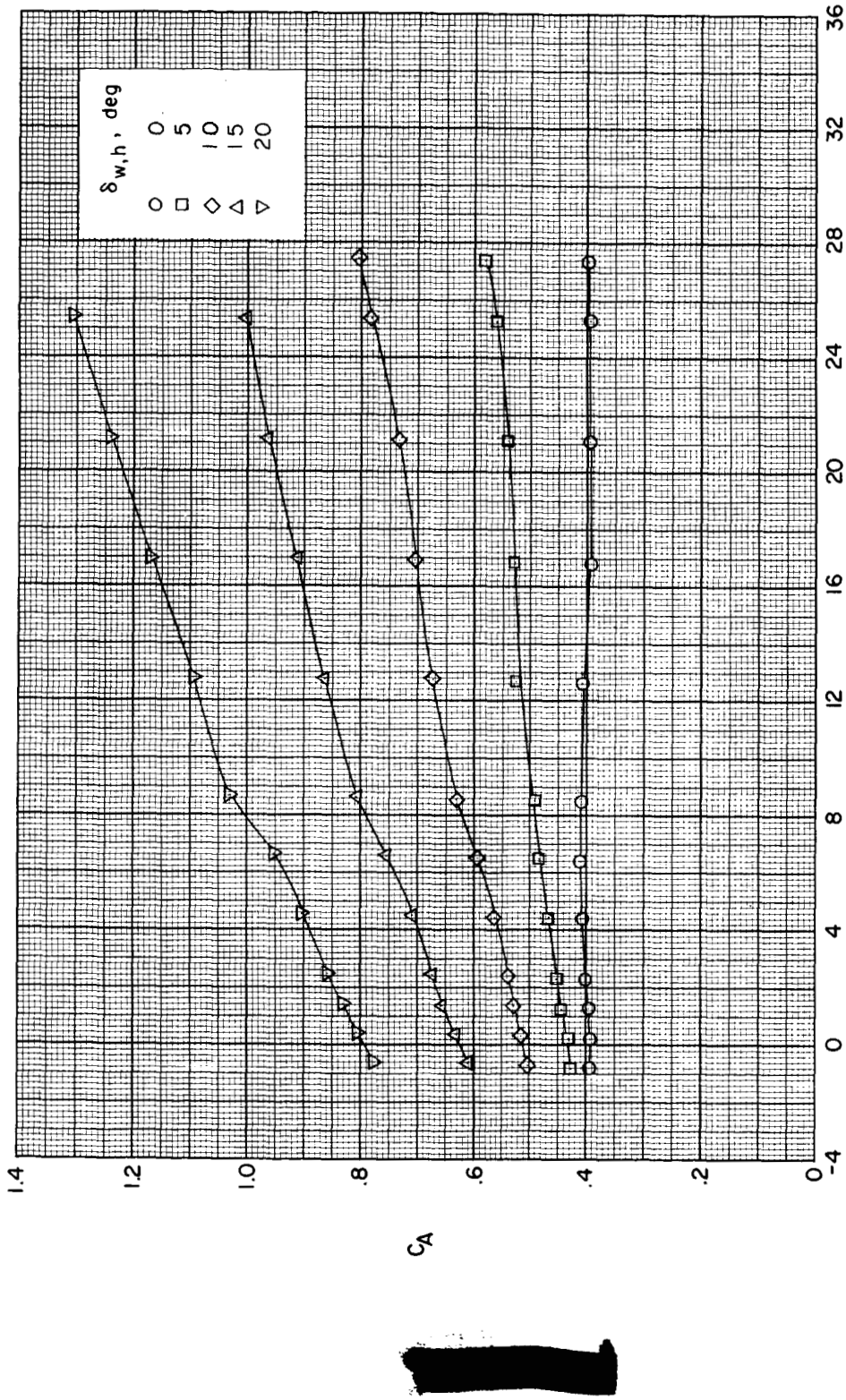

(a) Continued.

Figure 4.- Continued.

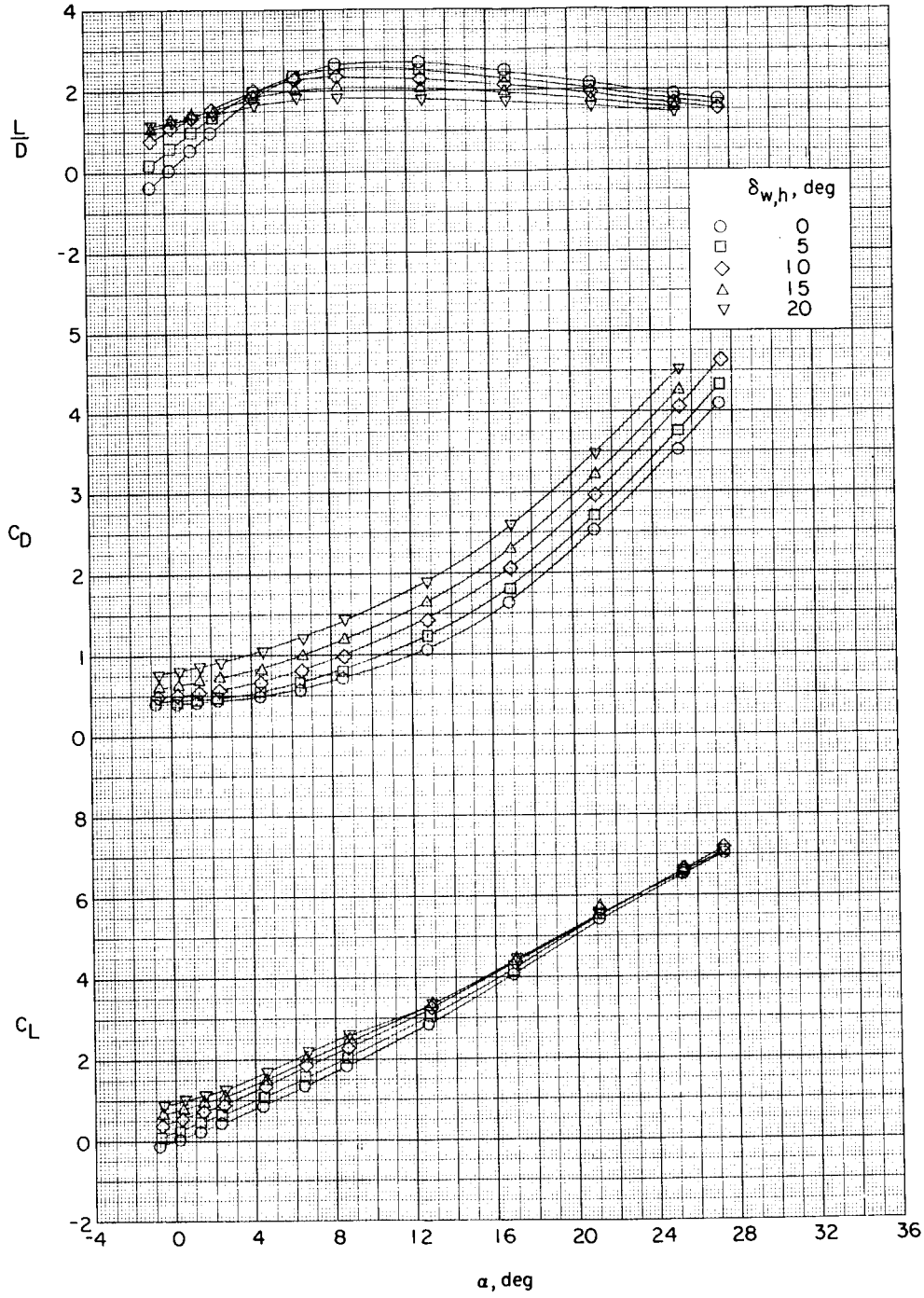

(a) Concluded.

Figure 4.- Continued.

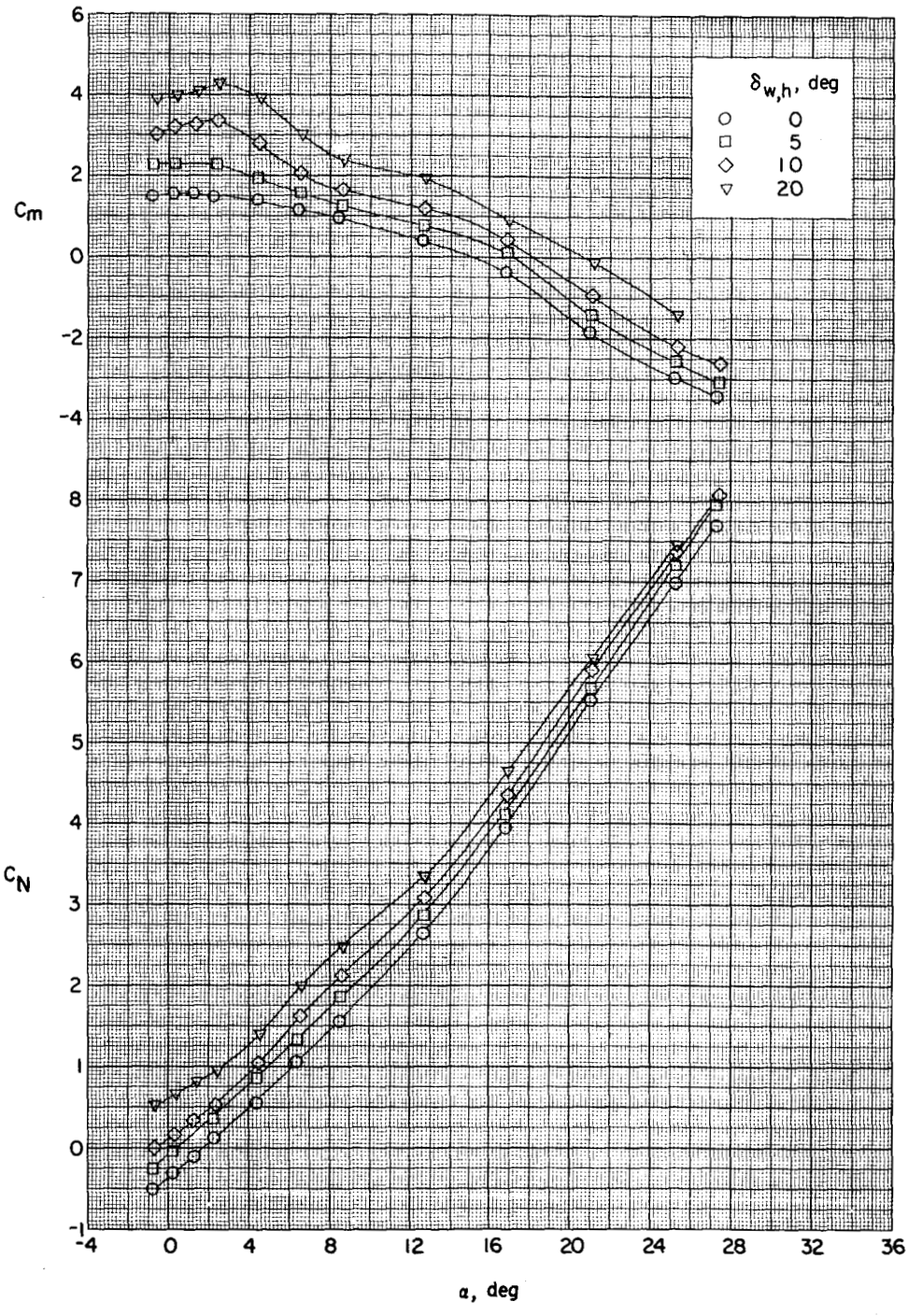

(b) $\delta_{t,h} = -10°$.

Figure 4.- Continued.

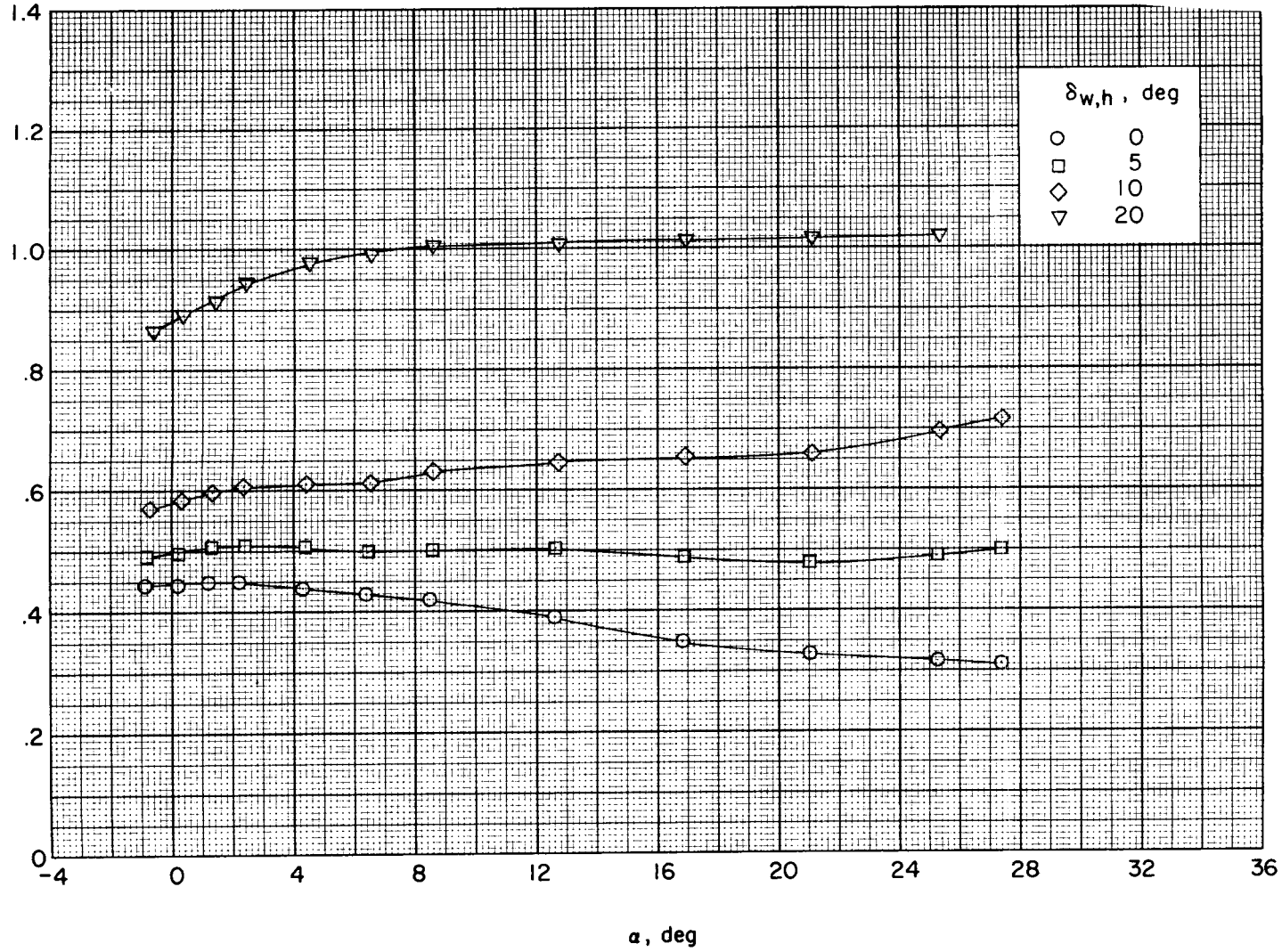

(b) Continued.

Figure 4.- Continued.

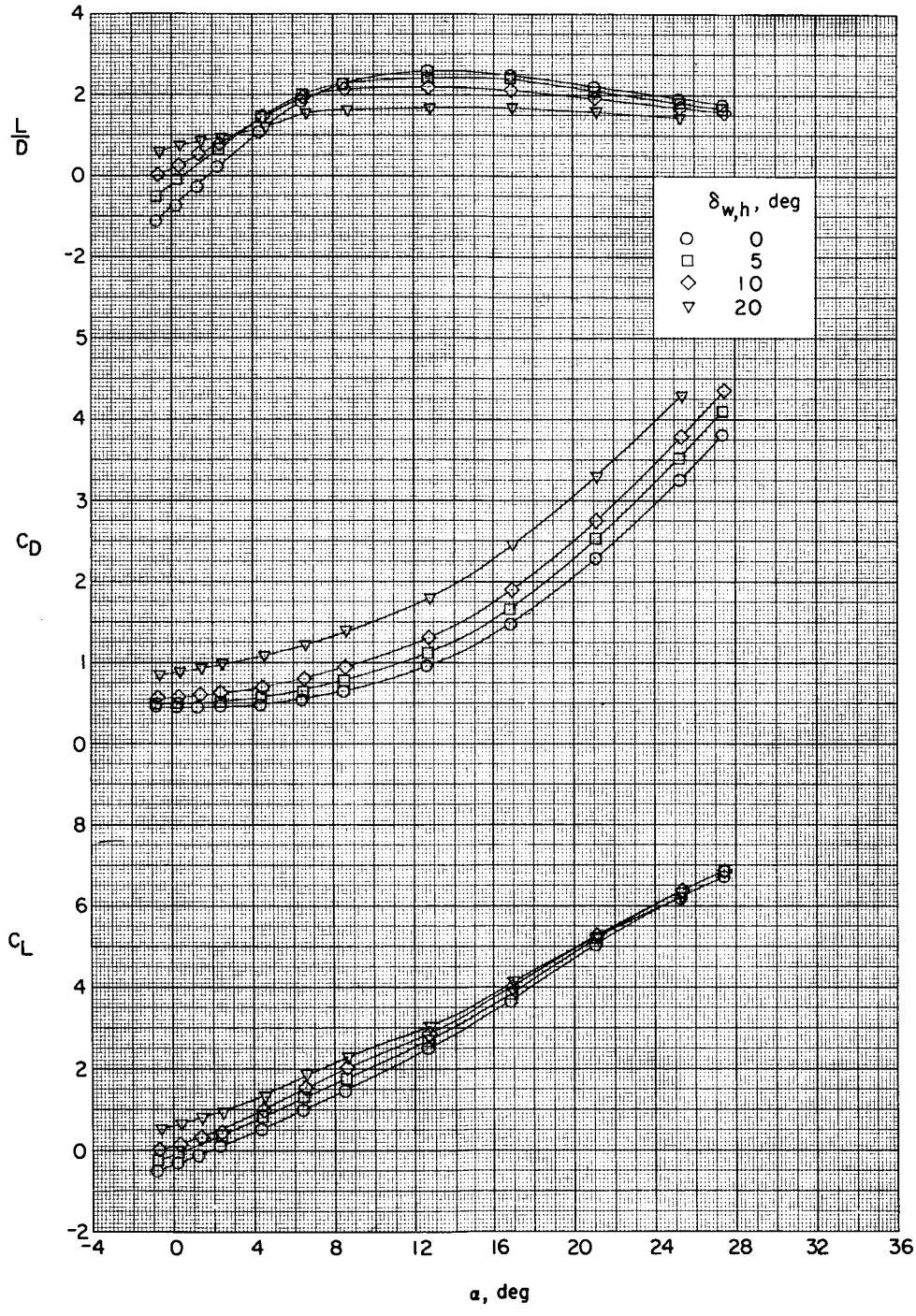

(b) Concluded.

Figure 4.- Continued.

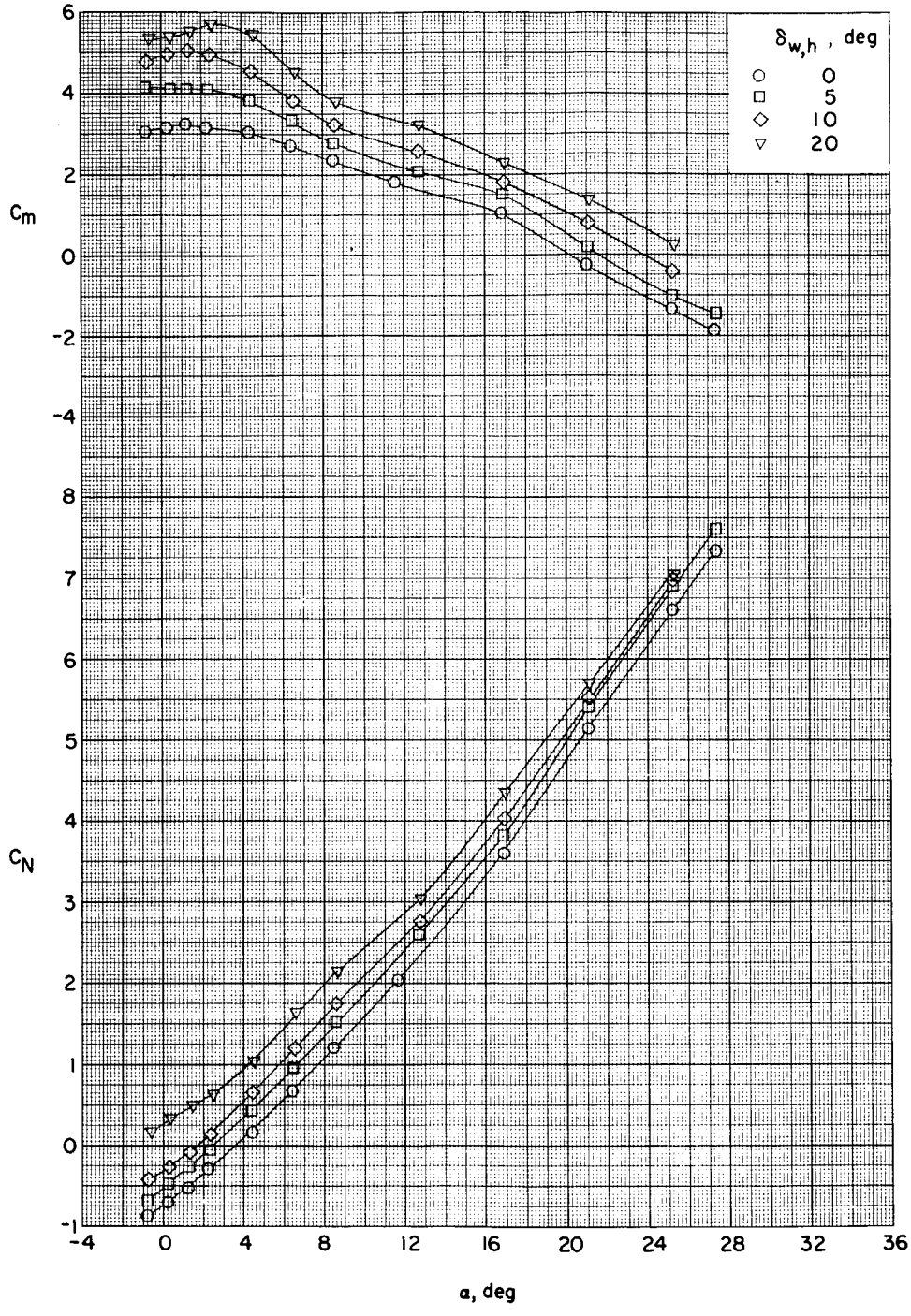

(c) $\delta_{t,h} = -20^\circ$.

Figure 4.- Continued.

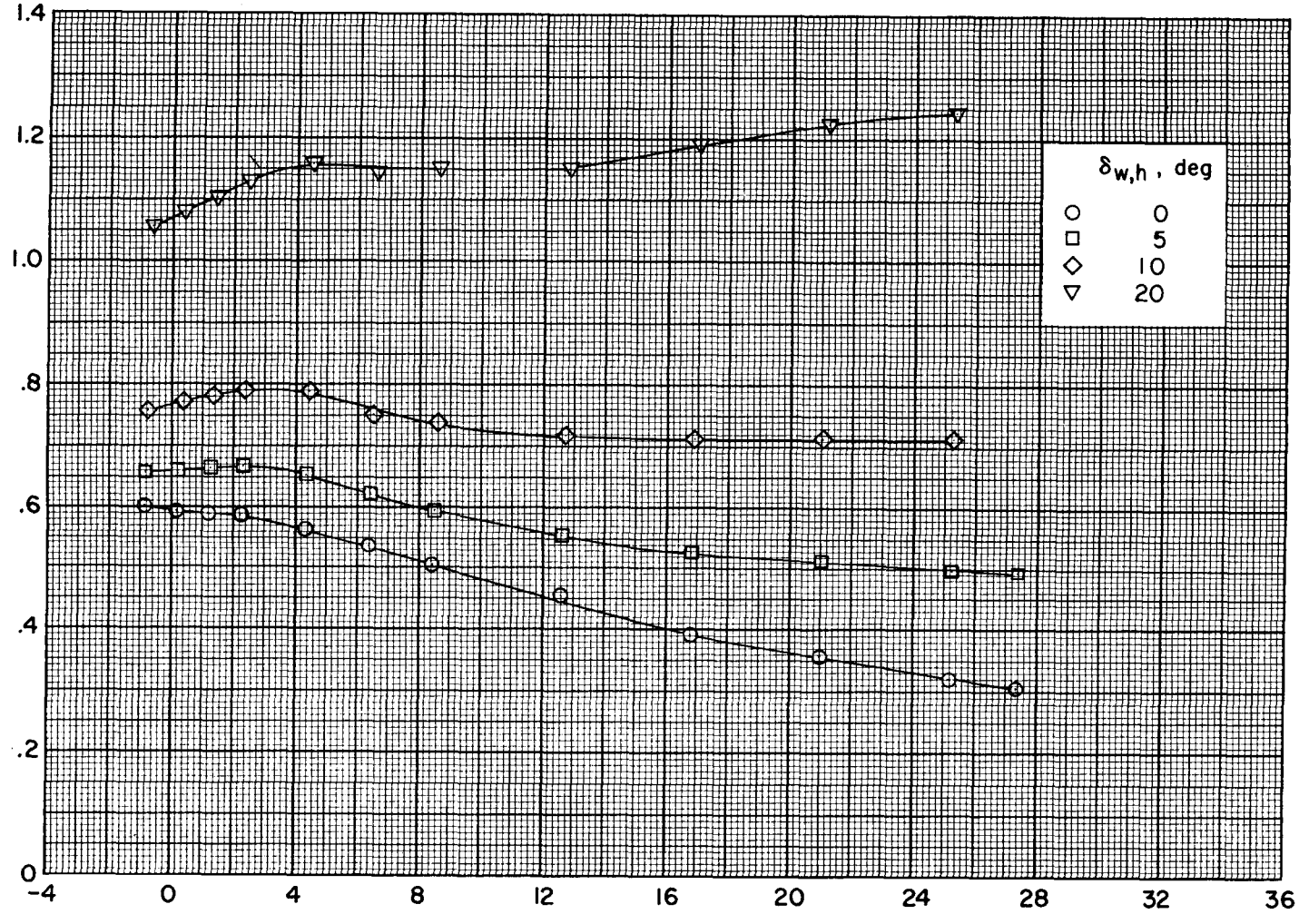

(c) Continued.

Figure 4.- Continued.

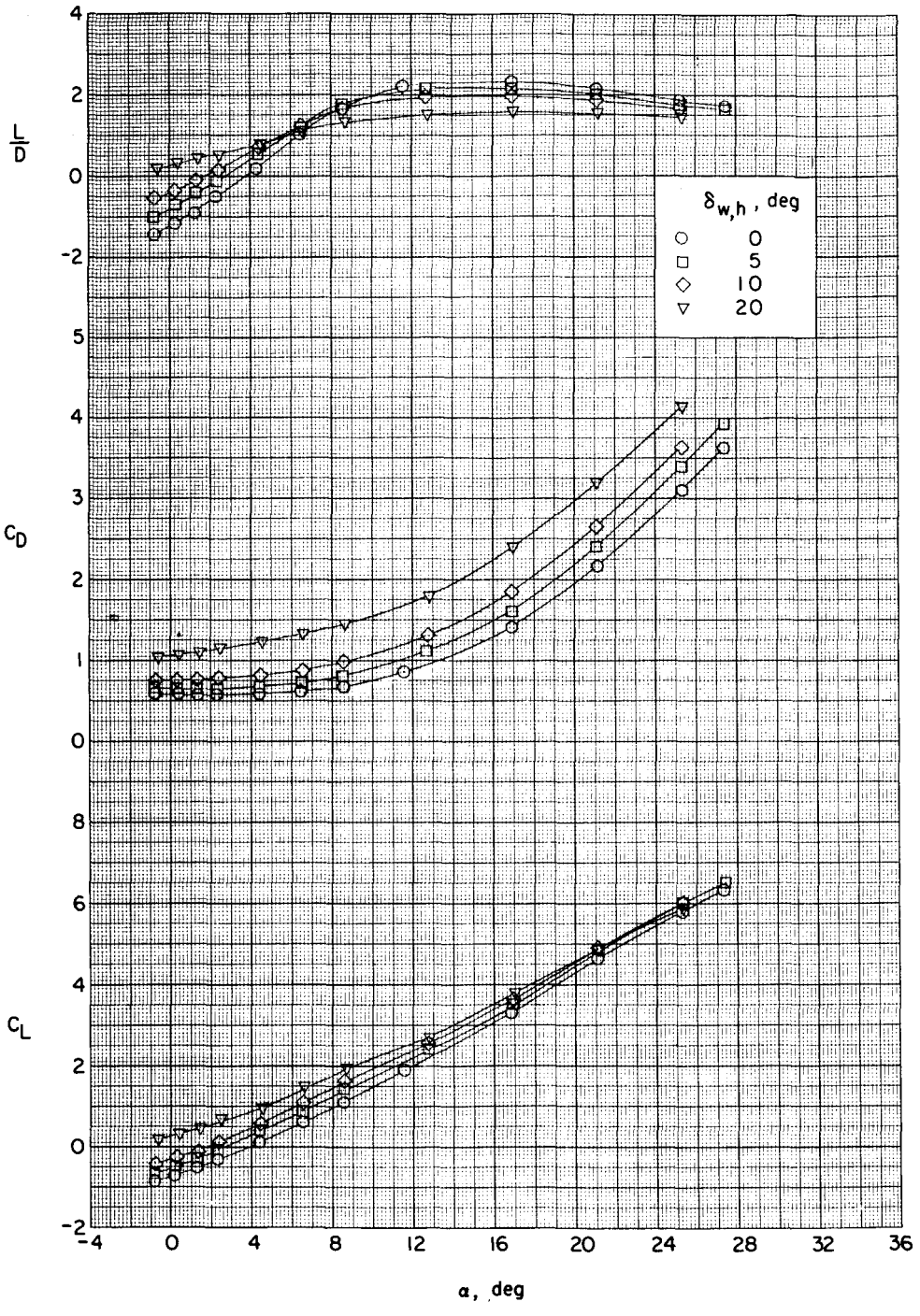

(c) Concluded.

Figure 4.- Concluded.

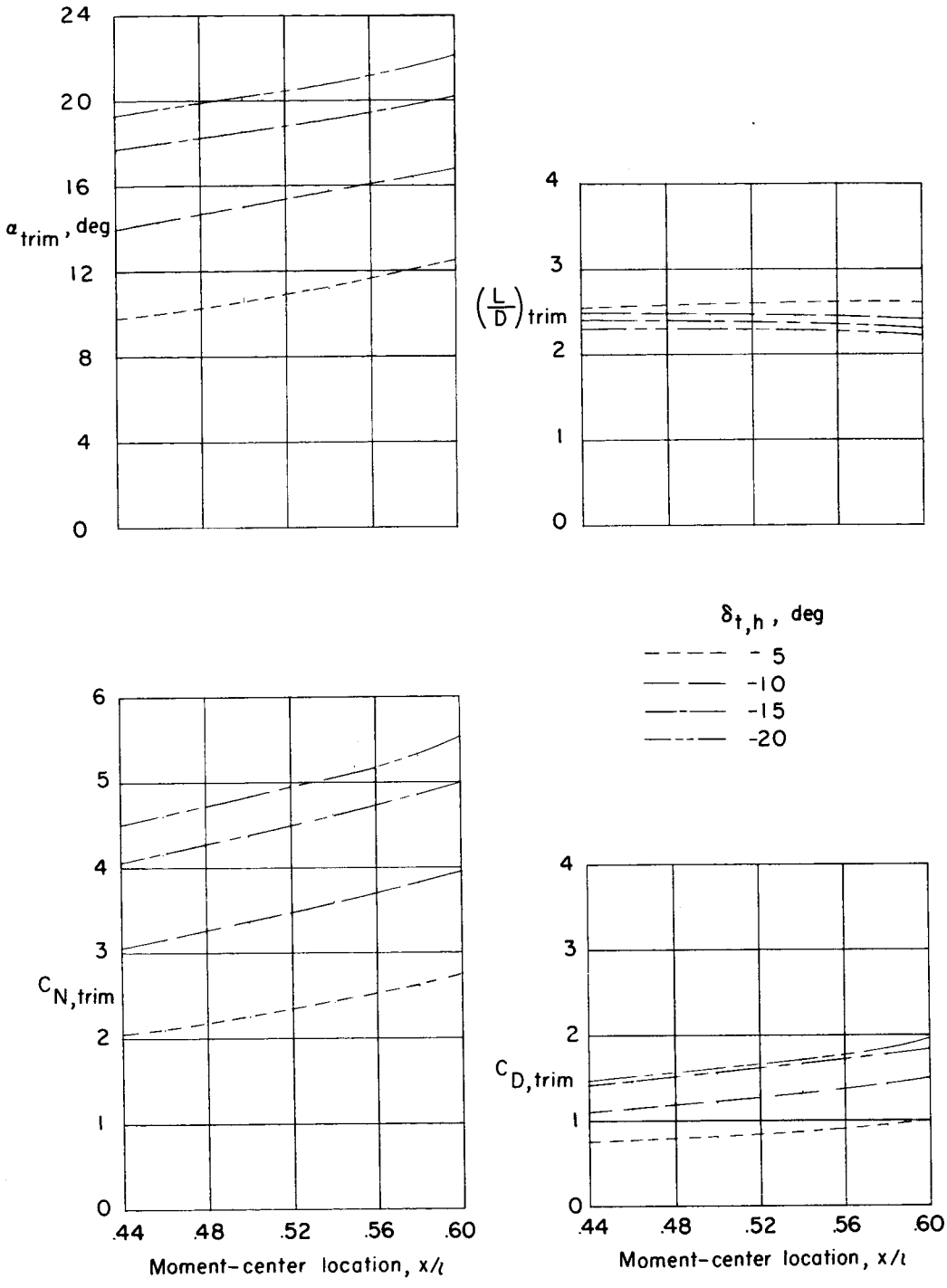

Figure 5.- Longitudinal trim characteristics for horizontal-tail controls. $\delta_w = 0^\circ$; $\delta_{t,v} = 0^\circ$.

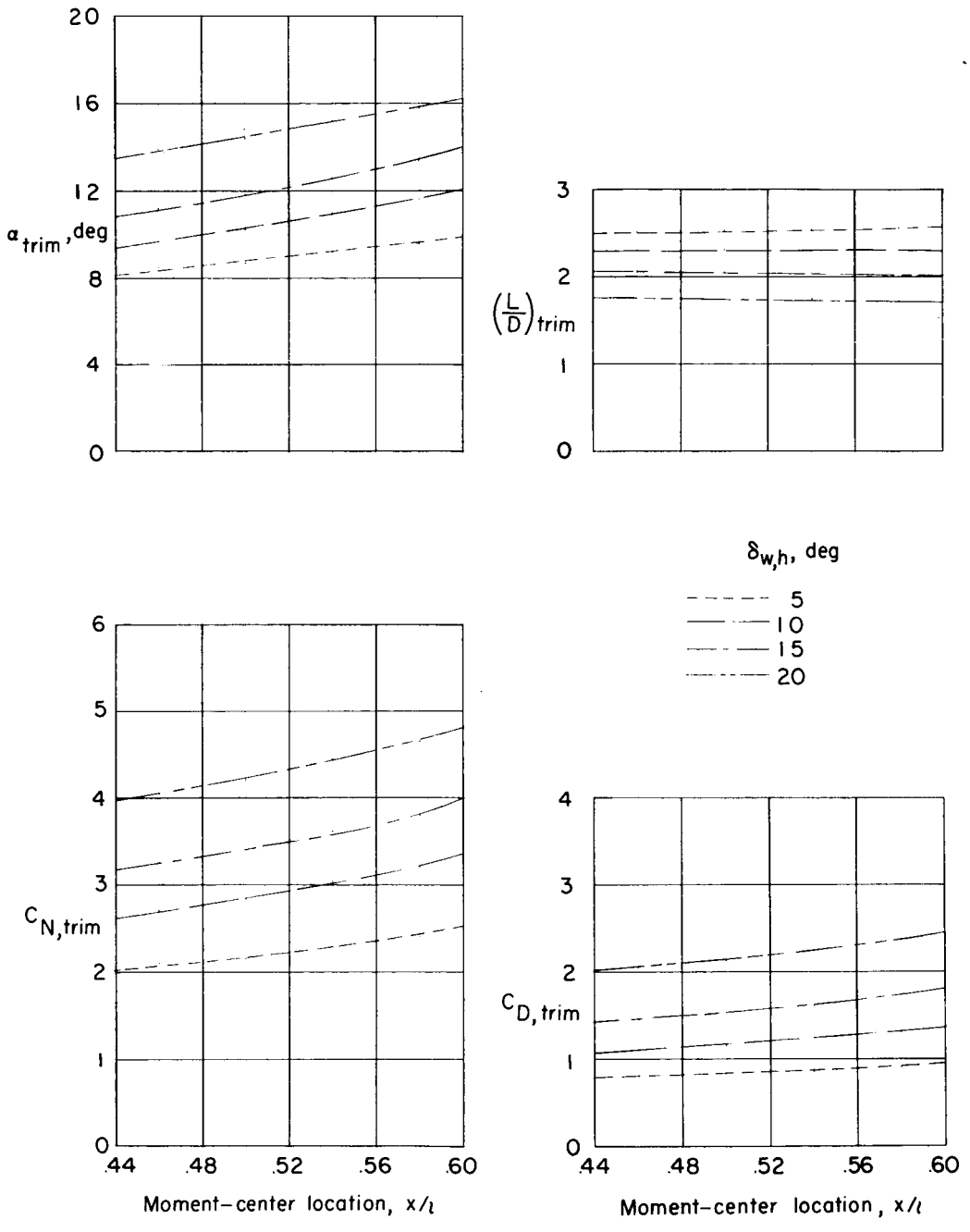

(a) $\delta_{t,h} = 0^{\circ}$.

Figure 6.- Longitudinal trim characteristics for wing controls at various deflections of horizontal tails. $\delta_{t,v} = 0^{\circ}$.

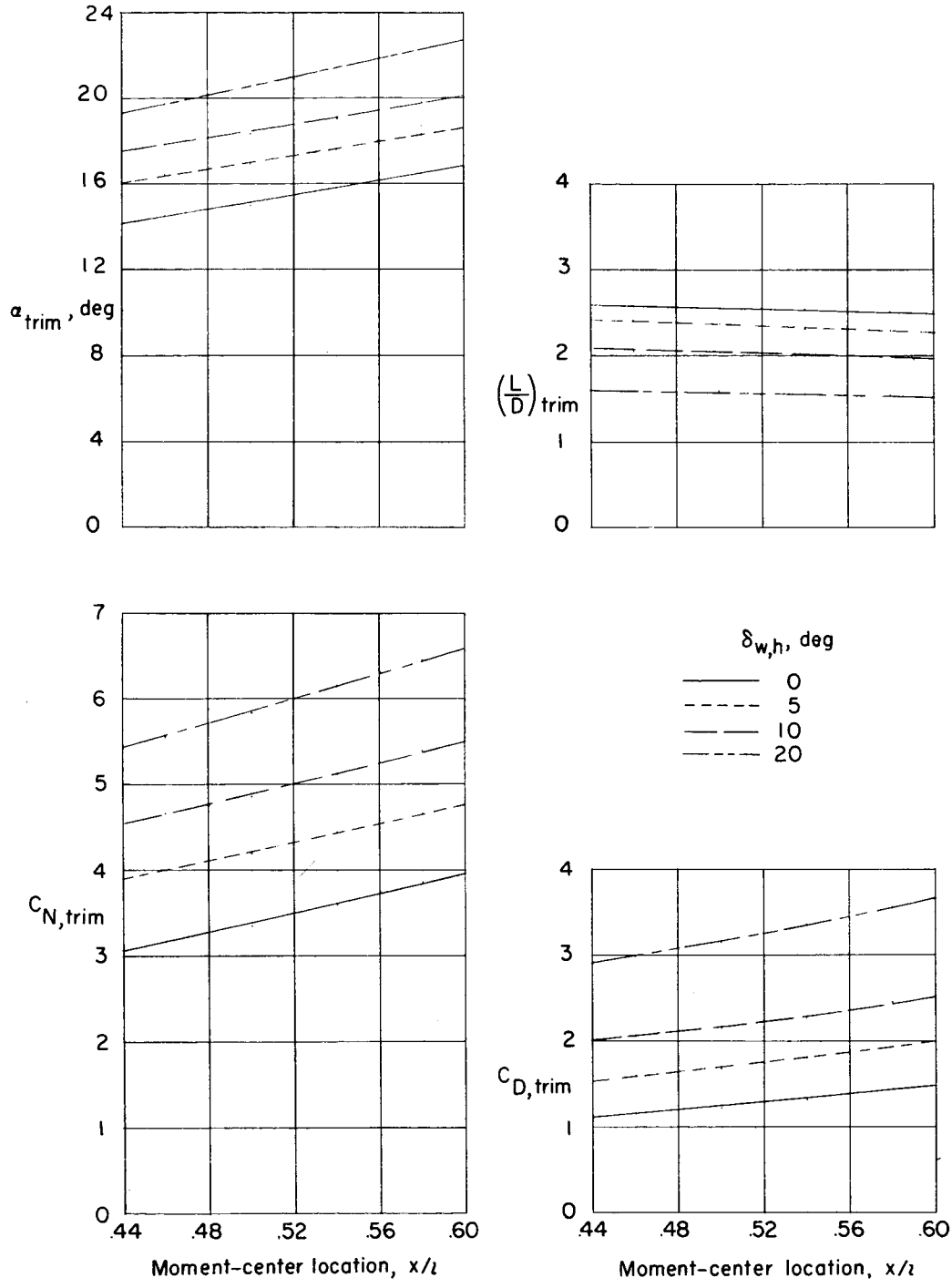

(b) $\delta_{t,h} = -10^{\circ}$.

Figure 6.- Continued.

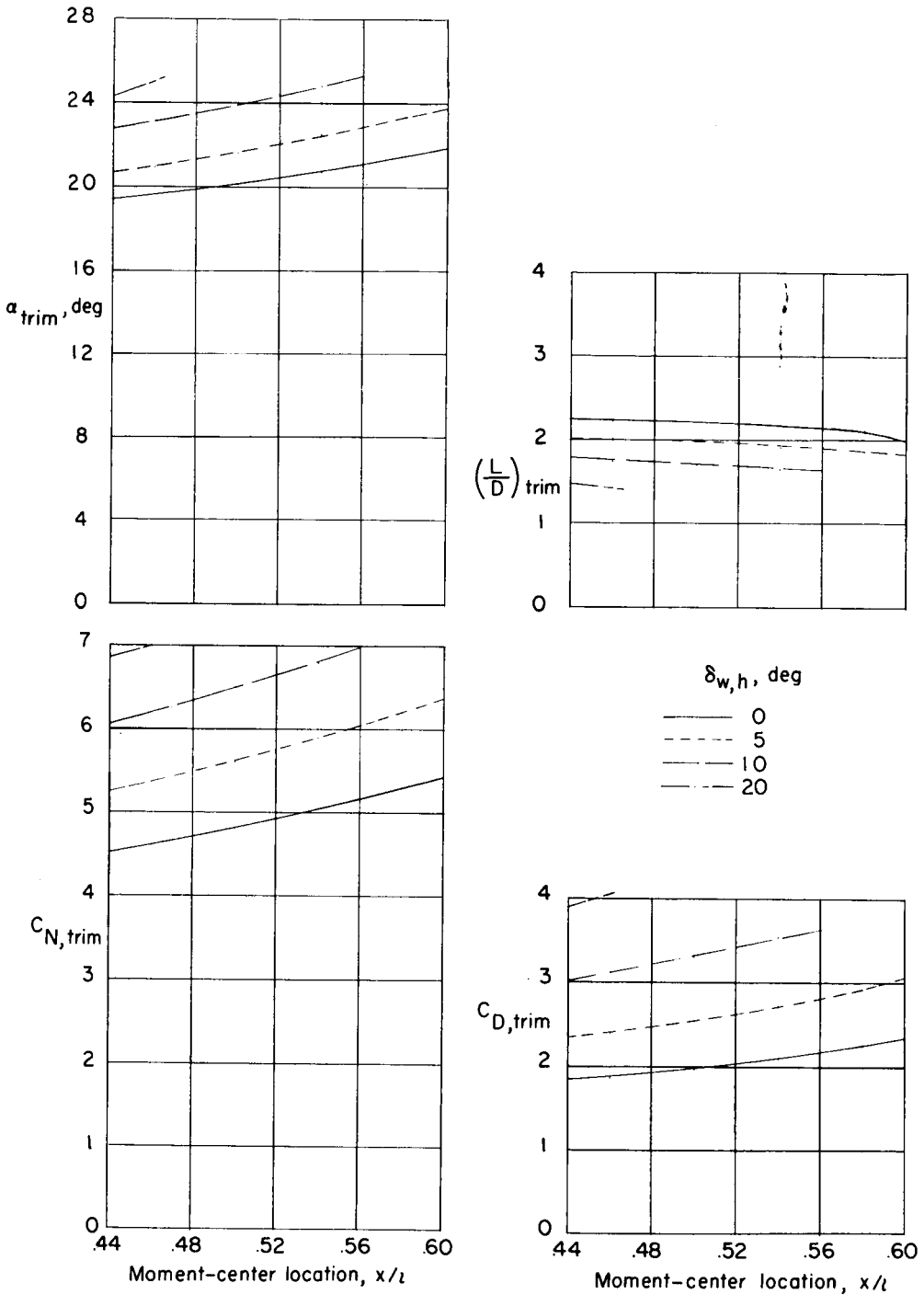

(c) $\delta_{t,h} = -20^{\circ}$.

Figure 6.- Concluded.

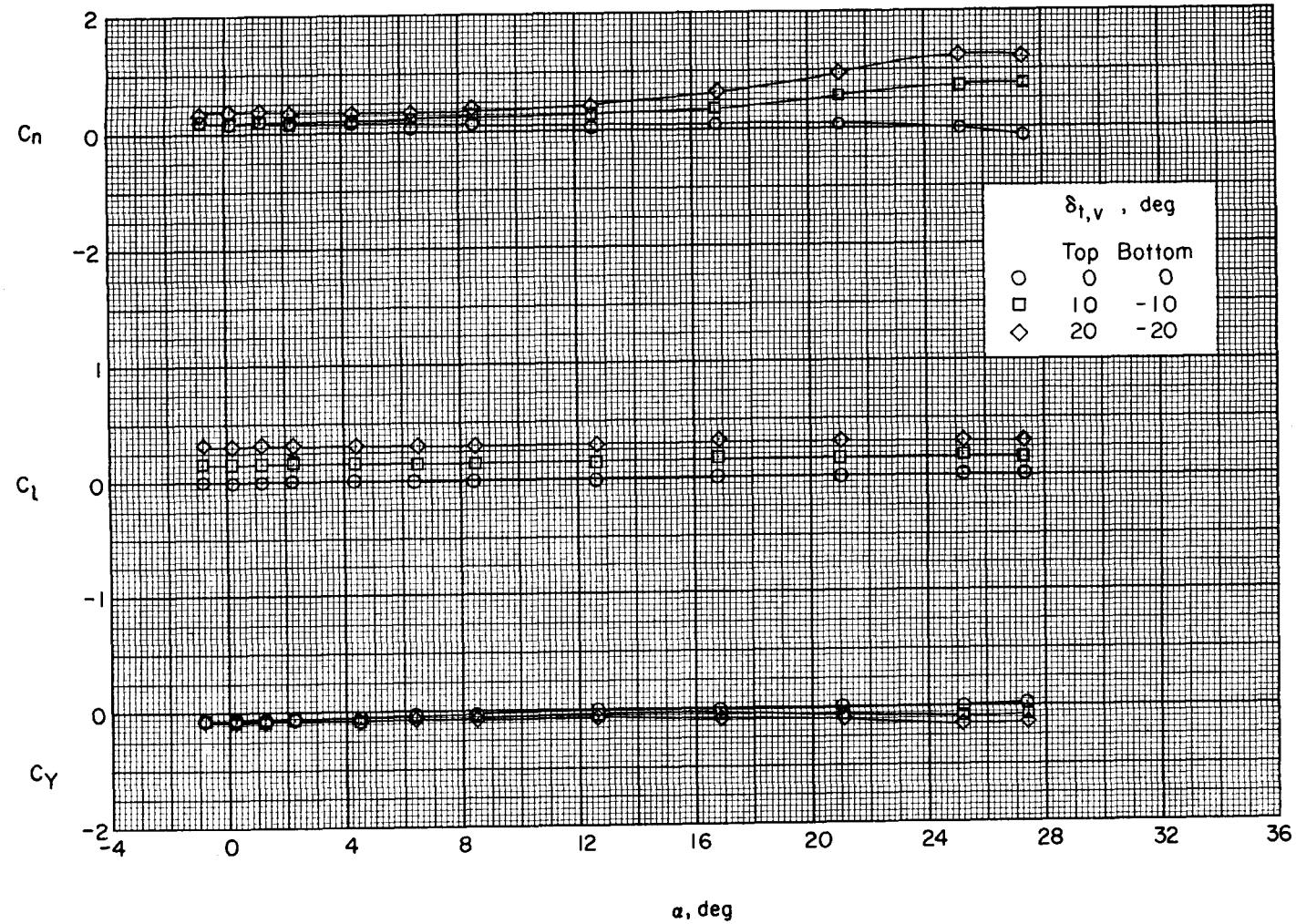

(a) Vertical-tail controls. $\delta_{w,v} = 0^\circ$.

Figure 7.- Roll control characteristics. $\delta_{w,h} = 0^\circ$; $\delta_{t,h} = 0^\circ$.

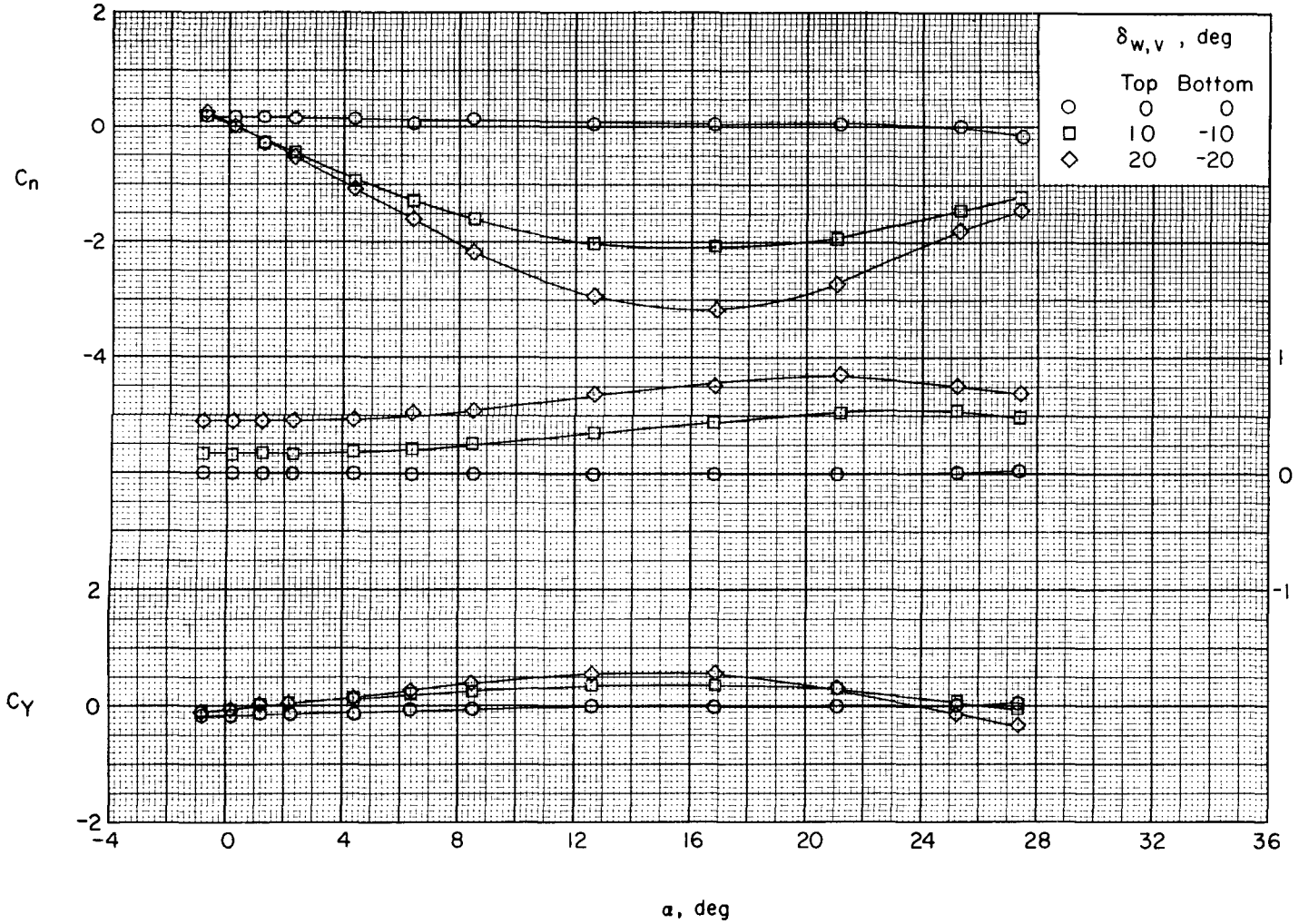

(b) Vertical-wing controls. $\delta_{t,v} = 0^\circ$.

Figure 7.- Concluded.

L-534